

Tennessee State University

Digital Scholarship @ Tennessee State University

Information Systems and Engineering
Management Research Publications

Center of Excellence in Information Systems
and Engineering Management

5-2000

64 Orionis: Three-Dimensional Orbit and Physical Parameters

Colin D. Scarfe
University of Victoria

David J. Barlow
University of Victoria

Francis C. Fekel
Tennessee State University

Follow this and additional works at: <https://digitalscholarship.tnstate.edu/coe-research>



Part of the [Stars, Interstellar Medium and the Galaxy Commons](#)

Recommended Citation

C. D. Scarfe et al 2000 AJ 119 2415

This Article is brought to you for free and open access by the Center of Excellence in Information Systems and Engineering Management at Digital Scholarship @ Tennessee State University. It has been accepted for inclusion in Information Systems and Engineering Management Research Publications by an authorized administrator of Digital Scholarship @ Tennessee State University. For more information, please contact XGE@Tnstate.edu.

64 ORIONIS: THREE-DIMENSIONAL ORBIT AND PHYSICAL PARAMETERS

C. D. SCARFE¹ AND D. J. BARLOW

Department of Physics and Astronomy, University of Victoria, Victoria, V8W 3P6, BC, Canada; scarfe@uvic.ca, barlow@uvic.ca

AND

FRANCIS C. FEKEL²

Center of Excellence in Information Systems, Tennessee State University, 330 Tenth Avenue North, Nashville, TN 37203-3401; fekel@coe.tnstate.edu

Received 1999 December 23; accepted 2000 February 4

ABSTRACT

We have obtained radial velocities of the components of the short-period subsystem of the B-type triple star 64 Orionis, covering a full cycle of the long-period orbit since the date of our earlier paper by Fekel & Scarfe. We use all of our radial velocities, together with available speckle interferometry, to derive a three-dimensional orbit for the long-period system. The system has orbital periods of 14.57213 days and 12.98 yr. We also determine spectroscopically a magnitude difference at 4500 Å of 1.0 ± 0.1 between the components of the close pair. Although radial velocities of the third component continue to elude us, we are able to derive masses and luminosities for all three components by requiring that they lie within the populated band of the observed mass-luminosity relationship. With this constraint, the orbital parallax is $0''.00374 \pm 0''.00017$. Our results are consistent with the spectral types and colors derived previously and with the *b* magnitude difference determined by earlier lunar occultation observations, within the uncertainties of those parameters.

Key words: binaries: general — stars: early-type — stars: individual (64 Orionis)

1. INTRODUCTION

The star 64 Orionis [HR 2130; HD 41040; McA 24; $\alpha = 06^{\text{h}}03^{\text{m}}27^{\text{s}}.4$, $\delta = 19^{\circ}41'26''$ (J2000.0); $V = 5.15$, $B - V = -0.11$, $U - B = -0.44$; B7] is a close triple system, consisting of three mid- or late-B stars, which has been observed with several different techniques including spectroscopy, lunar occultation, and speckle interferometry. From observations obtained at the Lick Observatory, Campbell (1922) announced that 64 Ori is a double-lined spectroscopic binary. Africano et al. (1976) discovered the third component of the system in an occultation observation, and McAlister & Hendry (1982) obtained the first speckle interferometric observation. Combining older velocities from the Lick Observatory with more recent ones from the McDonald Observatory and the Dominion Astrophysical Observatory (DAO), Fekel & Scarfe (1986) determined orbital periods of 14.572 days and 13.03 yr. Despite the small number of speckle observations that has resolved the components and the short section of the orbit that the observations cover, Mason (1997) was able to produce a visual orbit for the system with the help of the spectroscopic results.

The literature of efforts to determine the system's overall spectral type and color indices has been discussed by Fekel & Scarfe (1986). In summary, the spectral class is roughly B7 or B8 for both components of the close pair and about B5 or B6 for the distant component. There is no consensus on whether all the stars lie within the main-sequence band or whether one or both of the close pair fall slightly above it. The latter was suggested by Fekel & Scarfe (1986) as a way of reconciling the cooler types of the close pair with their

greater mass and luminosity. But this may also be possible within the width of the main sequence. The *UBV* colors are consistent with the types as they stand, without any correction for reddening, despite the presence of interstellar Ca II H and K lines in the spectrum.

We have obtained additional spectroscopic observations at DAO and the Kitt Peak National Observatory (KPNO), which cover a complete cycle of the long-period orbit. The full set of spectroscopic observations, combined with those from speckle interferometry, enable us to improve the orbital elements, particularly those of the long-period orbit, and to determine fairly reliably some of the fundamental parameters of the components. Following Fekel & Scarfe (1986), the short-period primary is component Aa and the secondary is Ab, both of which have narrow spectral features. They combine to form component A of the long-period pair. Component B of that system has very broad spectral features, as shown in Figure 3 of Fekel & Scarfe (1986).

2. OBSERVATIONS AND REDUCTIONS

In addition to the observations published in Table III of Fekel & Scarfe (1986), 48 photographic spectra, at a dispersion of 2.4 \AA mm^{-1} , have been obtained between 1983 and 1999 with the coude spectrograph of the DAO 1.2 m telescope. At least one spectrogram has been obtained in every observing season during that interval. They have been measured with the DAO ARCTURUS machine, which is controlled by the program SCRARC, and reduced with the program ARCREP, both developed by J. Murray Fletcher. The lines listed in Table II of Fekel & Scarfe (1986) have been used for these measurements. This in turn has required the continued use of photography, because the lines of shortest and longest wavelengths are focused about 30 cm apart, a distance greater than the size of any available electronic detector.

From 1983 to 1999, 40 spectroscopic observations were obtained at KPNO with the coude feed telescope and coude

¹ Guest Worker, Dominion Astrophysical Observatory, Herzberg Institute of Astrophysics, National Research Council of Canada.

² Visiting Astronomer, Kitt Peak National Observatory, National Optical Astronomy Observatories, which are operated by the Association of Universities for Research in Astronomy, Inc., under cooperative agreement with the National Science Foundation.

TABLE 1
RADIAL VELOCITY OBSERVATIONS

HJD (2,400,000 +)	ϕ_S	ϕ_L	V_{Aa} (km s ⁻¹)	V_{Ab} (km s ⁻¹)	γ_A (km s ⁻¹)	$(O-C)_{Aa}$ (km s ⁻¹)	$(O-C)_{Ab}$ (km s ⁻¹)
New DAO data:							
45,603.003.....	0.362	0.225	-12.1	33.9	9.8	-0.1	1.0
45,691.907.....	0.463	0.244	-3.4	24.4	9.8	-0.4	0.3
45,735.758.....	0.472	0.253	-0.7	23.5	10.8	1.2	0.1
45,812.693.....	0.751	0.270	30.1	-11.9	10.1	-0.7	0.0
45,973.965.....	0.819	0.304	42.1	-22.5	11.4	0.4	-0.1
46,036.859.....	0.135	0.317	-15.2	40.3	11.2	-0.2	-0.4
46,099.646.....	0.443	0.330	-2.8	27.9	11.8	0.1	0.0
46,161.684.....	0.701	0.343	25.4	-2.3	12.2	0.2	0.3
46,381.930.....	0.815	0.390	43.2	-20.6	12.9	0.5	-0.4
46,465.755.....	0.567	0.407	13.0	2.5 ^a	...
46,520.725.....	0.340	0.419	-9.2	38.7	13.6	0.5	0.1
46,660.006.....	0.898	0.448	54.4	-32.1	13.3	0.2	-1.1
46,886.649.....	0.451	0.496	0.4	30.7	14.8	-0.0	0.9
47,042.980.....	0.179	0.529	-14.1	47.5	15.2	0.3	0.4
47,089.917.....	0.400	0.539	-3.6	35.9	15.2	-0.2	0.7
47,218.688.....	0.237	0.566	-12.0	47.8	16.4	1.4	0.8
47,428.911.....	0.663	0.610	25.2	6.3	16.2	0.9	-0.4
47,499.941.....	0.537	0.625	10.8	22.5	16.4	0.4	0.1
47,583.654.....	0.282	0.643	-10.3	46.3	16.6	0.0	0.6
47,792.960.....	0.646	0.687	23.3	11.0	17.5	0.1	1.0
47,815.906.....	0.220	0.692	-12.4	48.6	16.6	-0.2	-0.6
47,871.931.....	0.065	0.704	7.1	28.8	17.4	0.2	-0.4
47,941.656.....	0.850	0.719	52.1	-21.4	17.1	-0.3	-0.0
48,158.973.....	0.763	0.764	40.4	-5.9	18.4	0.4	0.4
48,277.677.....	0.909	0.789	60.1	-27.4	18.5	0.7	-0.3
48,325.683.....	0.203	0.800	-10.4	50.0	18.3	0.6	-0.8
48,514.963.....	0.192	0.839	-10.0	51.2	19.1	0.4	-0.2
48,690.739.....	0.255	0.877	-8.5	50.8	19.7	0.1	0.5
49,036.745.....	0.999	0.950	40.3	-5.2	18.7	0.1	-0.0
49,073.715.....	0.536	0.957	13.1	25.6	19.0	1.0	1.2
49,082.672.....	0.151	0.959	-10.4	48.9	17.8	-0.2	0.4
49,229.988.....	0.260	0.990	-20.4	37.5	7.1	0.4	-0.1
49,241.958.....	0.082	0.993	-10.3	22.6	5.3	0.5	-0.3
49,246.971.....	0.426	0.994	-12.1	22.2	4.2	-0.5	-0.1
49,264.995.....	0.663	0.998	10.4	-7.3	2.0	0.2	0.1
49,303.927.....	0.334	0.006	-26.7	23.5	-2.8	-0.6	0.5
49,358.737.....	0.096	0.017	-24.6	16.4	-5.1	0.1	-0.6
49,383.663.....	0.806	0.023	24.3	-35.4	-4.1	0.3	0.7
49,418.631.....	0.206	0.030	-32.6	28.4	-3.6	0.5	-0.3
49,614.988.....	0.681	0.071	12.1	-8.1	2.5	-0.1	2.0
49,739.767.....	0.244	0.098	-24.9	34.7	3.4	-0.2	-0.5
49,977.006.....	0.524	0.148	-0.1	16.1	7.6	0.3	1.7
50,145.641.....	0.096	0.183	-12.5	28.6	7.0	-0.6	-1.5
50,510.671.....	0.146	0.260	-17.1	40.5	10.3	0.2	-0.2
50,714.005.....	0.100	0.303	-10.1	34.5	11.1	-0.5	-0.4
50,879.716.....	0.472	0.338	-2.0	23.5	10.1	-1.8	-1.7
51,083.978.....	0.489	0.381	1.6	22.9	11.7	-0.6	-1.3
51,444.010.....	0.196	0.457	-17.1	47.3	13.5	-1.5	1.0
New KPNO data:							
45,449.652.....	0.838	0.193	43.2	-28.4	9.2	1.4	0.0
45,450.614.....	0.904	0.193	53.0	-34.5	11.4 ^b	3.7 ^a	2.2
45,451.617.....	0.973	0.193	44.0	-25.9	10.8	2.9 ^a	1.8
45,595.945.....	0.877	0.224	49.5	-32.7	10.4	1.5	0.6
45,596.916.....	0.944	0.224	49.4	-35.0	9.3	0.5	-0.7
45,717.679.....	0.231	0.249	-19.1	41.2	9.6	-0.2	-0.7
45,718.663.....	0.299	0.250	-15.2	39.2	10.7	0.5	0.9
45,814.640.....	0.885	0.270	50.1	-33.2	10.5	0.1	-0.2
46,390.827.....	0.425	0.391	-2.8	31.6	13.6	0.6	1.0
46,718.935.....	0.942	0.461	53.8	-30.2	13.9	0.0	-0.1
46,721.878.....	0.144	0.461	-13.4	44.6	14.2	0.1	0.6
47,248.716.....	0.297	0.572	-9.5	42.8	15.4	0.9	-1.0
47,458.878.....	0.721	0.617	32.4	0.3	17.1	0.6	1.7
47,625.636.....	0.163	0.652	-12.3	48.4	16.6	-0.1	0.3

TABLE 1—Continued

HJD (2,400,000 +)	ϕ_S	ϕ_L	V_{Aa} (km s ⁻¹)	V_{Ab} (km s ⁻¹)	γ_A (km s ⁻¹)	$(O-C)_{Aa}$ (km s ⁻¹)	$(O-C)_{Ab}$ (km s ⁻¹)
47,810.880.....	0.875	0.691	55.8	-26.2	16.8	0.4	-0.8
47,814.898.....	0.151	0.692	-11.4	48.3	17.0	-0.4	0.5
47,917.780.....	0.211	0.714	-12.0	48.8	16.9	0.1	-0.8
48,003.618.....	0.102	0.732	-4.4	40.4	16.9	-0.7	-0.5
48,167.884.....	0.374	0.766	-1.2	40.3	18.5	1.2	0.1
48,573.869.....	0.235	0.852	-8.7	51.6	20.0	1.0	0.7
48,916.891.....	0.774	0.924	43.7	-6.7	19.7	0.5	-0.1
49,105.618.....	0.726	0.964	34.2	-0.2	17.8	0.5	1.1
49,246.991.....	0.427	0.994	-11.9	23.1	4.7	-0.4	1.0
49,251.940.....	0.767	0.995	25.4	-20.6	3.5	-0.9	0.6
49,344.749.....	0.136	0.014	-32.1	28.3	-3.4	-0.8	3.7 ^a
49,344.754.....	0.136	0.014	-30.9	25.0	-4.3	0.5	0.4
49,382.582.....	0.732	0.022	12.7	-23.4	-4.5	-0.2	0.6
49,383.661.....	0.806	0.023	23.9	-36.8	-5.0	-0.0	-0.7
49,462.607.....	0.224	0.039	-31.6	28.6	-3.0	-0.1	-1.1
49,622.938.....	0.226	0.073	-26.8	34.6	2.4	0.5	0.8
49,677.887.....	0.997	0.085	25.2	-24.4	1.6	0.2	-2.2
49,836.622.....	0.890	0.118	46.2	-38.8	5.8	1.1	0.1
49,973.934.....	0.313	0.147	-18.5	34.1	6.5	-0.4	0.1
50,203.622.....	0.075	0.196	-6.0	23.5	8.0	-0.5	-0.4
50,366.880.....	0.279	0.230	-17.8	37.2	8.4	-0.5	-0.9
50,404.794.....	0.881	0.238	49.7	-32.8	10.5	1.0	0.5
50,758.798.....	0.174	0.313	-17.8	44.0	11.6	-0.1	0.5
50,833.677.....	0.312	0.329	-12.5	40.3	12.6	0.6	1.2
51,088.935.....	0.829	0.382	44.8	-22.8	12.7	0.1	-0.1
51,307.620.....	0.836	0.428	47.0	-24.2	13.1	0.5	-1.1

^a 3 σ residual, velocity not used in solution.

^b 3 σ residual, not plotted in Fig. 2.

spectrograph. Three spectra, having a central wavelength of 6375 Å, a wavelength range of 65 Å, and a resolution of 0.30 Å, were taken with a RCA CCD detector during 1983 April. In 1993 December and 1994 January, four spectra, having a central wavelength of 4505 Å, a wavelength range of 170 Å, and a resolution of 0.30 Å, were acquired with a Tektronix CCD. The rest of the spectra, obtained with a Texas Instruments CCD, are centered at 4500 Å, cover a wavelength range of just over 80 Å and have a resolution of 0.21 Å. This wavelength region includes the He I line at 4471.477 Å, the Mg II line at 4481.228 Å, and several Fe II lines redward of the Mg II line. The spectra have typical signal-to-noise ratios (S/N) of 200–300.

The 4481 Å Mg II absorption feature of component B is visible in the relatively high-S/N CCD spectra (see Fig. 3 of Fekel & Scarfe 1986). However, accurate velocity measurement of this component is not possible because of its broad-lined nature and the superposition of lines from Aa and Ab. Radial velocities of Aa and Ab were determined with the procedure of Fekel, Bopp, & Lacy (1978) or by cross-correlation with the IRAF program FXCOR (Fitzpatrick 1993). Several spectra were measured with both techniques, and no systematic difference was found between the results. Because the Mg II line is much stronger than any other metal lines in the observed blue-wavelength region, velocities for Aa and Ab were measured for this line alone. In addition, a mean velocity for each component was determined from four to five of the much weaker Fe II lines. Usually the velocities of the Mg II and the several Fe II lines were averaged to produce final velocities for Aa and Ab. In a few cases, the Mg II lines of Aa and Ab were too blended, so only the mean velocity of the weak metal lines was used

for each component. The primary velocity standard was 68 Tau, although HR 3383 or θ Leo was sometimes used. Velocities for those stars, adopted from Fekel (1999), are 39.0, 2.8, and 7.4 km s⁻¹, respectively. All our new radial velocities are set out in Table 1, which follows the style of Table III of Fekel & Scarfe (1986).

3. ORBITAL SOLUTION

Following the example of Mason (1997), we have made use of the eight Center for High Angular Resolution Astronomy (CHARA) speckle observations (from Hartkopf, McAlister, & Mason's 1999 Third Catalogue of Interferometric Measurements of Binary Stars)³ only, since they are a homogeneous set; they are listed for reference in Table 2. A simultaneous solution of those data, together with all of our radial velocities, has been found, with the three-dimensional differential correction program (Fekel et al. 1997) developed by one of us (D. J. B.). Preliminary solutions of the radial velocities alone showed that the effect of applying light-time corrections to the times of the observations is negligible on either the elements or their uncertainties. Such corrections reduce the sum of the weighted squares of residuals by only a statistically insignificant 7%, and none have therefore been used in the final solution. Moreover, no improvement in the precision of the periods was achieved by including observations other than our own; hence, nor have those older data been used. To equalize zero points, we have added 0.3 km s⁻¹ to all the

³ Available at <http://www.chara.gsu.edu/CHARA/DoubleStars/Speckle/intro.html>.

TABLE 2
SPECKLE INTERFEROMETRIC OBSERVATIONS

Date (Besselian yr)	Phase	θ_{obs} (deg)	$(O-C)_\theta$ (deg)	ρ_{obs} (arcsec)	$(O-C)_\rho$ (arcsec)	Weight
1977.1798.....	0.720	64.4	-2.7	0.066	0.006	0.5
1977.7340.....	0.763	66.3	2.0	0.054	-0.004	1.0
1977.9142.....	0.777	64.7	1.4	0.069	0.012	0.5
1979.0364.....	0.863	55.4	-0.6	0.048	0.001	1.0
1986.8865.....	0.468	84.7	0.6	0.053	0.000	1.0
1988.2491.....	0.573	77.4	1.0	0.056	-0.003	1.0
1988.6637.....	0.605	72.8	-1.6	0.054	-0.006	1.0
1990.7555.....	0.766	63.3	-0.8	0.063	0.005	1.0

McDonald Observatory observations and 1.6 km s^{-1} to the two DAO observations at 6.5 \AA mm^{-1} that are listed by Fekel & Scarfe (1986). We have retained the weighting scheme adopted by Fekel & Scarfe (1986); in it, all the new observations of the primary star, Aa, were given weight 3.0, and all velocities of the secondary, Ab, received half the weight given to the corresponding primary-star velocity. Because the radial velocities are much more numerous than the speckle data, all the elements are essentially those that would be derived from the radial velocities alone, except for those obtainable only from the speckle data, namely, a , i_L , and Ω .

Starting values of the elements were taken from Fekel & Scarfe (1986) and Mason (1997). The final ones, along with the projected major semiaxes and the directly derivable mass information, are presented in Table 3. It may be noted that the uncertainties of almost all the spectroscopic elements have been reduced by a factor close to 2 from those presented in Table IV of Fekel & Scarfe (1986). That of the long period itself has been reduced by a larger factor, nearly 4. This is not surprising, since for our earlier paper our own observations did not cover a full cycle of the long period; now, by contrast, they cover nearly two cycles. The elements have been used to subtract the long-period variation from the data, and the residuals are plotted against the short-period phase, ϕ_S , in Figure 1. The ratio of the short-

period amplitudes,

$$q = \frac{K_{\text{Aa}}}{K_{\text{Ab}}} = 0.9068 \pm 0.0035, \quad (1)$$

can be used to provide an estimate of the short-period systemic velocity from each pair of velocities, V_{Aa} and V_{Ab} , by means of the expression

$$\gamma_A = V_{\text{Aa}} + \frac{q(V_{\text{Ab}} - V_{\text{Aa}})}{1 + q}. \quad (2)$$

Values of γ_A calculated this way are given in the sixth column of Table 1 and are plotted against the long-period phase, ϕ_L , in Figure 2. Comparison of that figure with Figure 2 of Fekel & Scarfe (1986) shows that our coverage of the phases near periastron has improved significantly. However, the long period is about a week less than 13 yr, and consequently it will be several decades before the remaining phase gap can easily be filled in.

Figure 3 shows the ellipse that represents the visual elements, obtained from our three-dimensional solution (Table 3), compared with the speckle interferometric observations. Our elements are similar to those of Mason (1997) but with uncertainties smaller by factors of 2–3. As shown in Figure 3, even with telescopes as large as 4 m, the visual components are unresolvable over much of the orbit. However,

TABLE 3
ORBITAL ELEMENTS

Parameter	Short Period	Long Period
P (days).....	14.572128 ± 0.000022	4741.1 ± 5.2
P (yr).....	...	12.980 ± 0.014
T (HJD).....	$2,443,164.188 \pm 0.011$	$2,444,535.0 \pm 5.5$
T (yr).....	...	1980.812 ± 0.015
γ (km s^{-1}).....	...	12.607 ± 0.052
K_{Aa} (km s^{-1}).....	35.353 ± 0.087	...
K_{Ab} (km s^{-1}).....	38.99 ± 0.12	...
K_A (km s^{-1}).....	...	12.224 ± 0.099
e	0.3870 ± 0.0019	0.7407 ± 0.0042
ω (deg).....	64.32 ± 0.31	305.30 ± 0.71
Ω (deg).....	...	230.1 ± 1.5
i (deg).....	...	115.7 ± 2.2
a (arcsec).....	...	0.0471 ± 0.0017
$a_{\text{Aa}} \sin i$ (Gm).....	6.532 ± 0.017	...
$a_{\text{Ab}} \sin i$ (Gm).....	7.204 ± 0.023	...
$a_A \sin i$ (Gm).....	...	535.4 ± 5.7
$\mathcal{M}_{\text{Aa}} \sin^3 i$ (\mathcal{M}_\odot).....	0.2553 ± 0.0018	...
$\mathcal{M}_{\text{Ab}} \sin^3 i$ (\mathcal{M}_\odot).....	0.2315 ± 0.0015	...
f (\mathcal{M}_\odot).....	...	0.2727 ± 0.0087

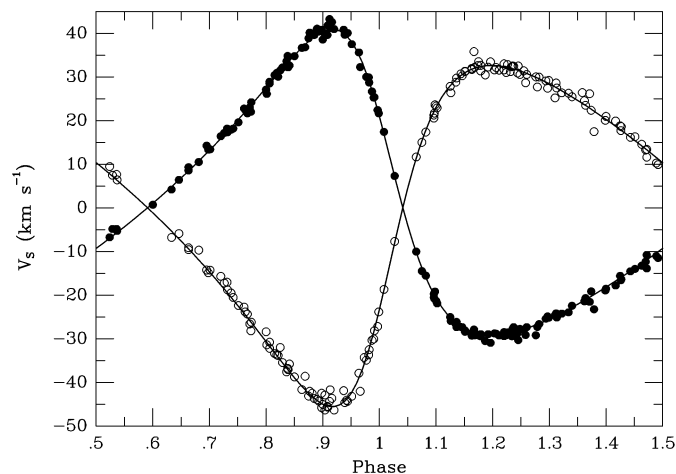


FIG. 1.—Radial velocities of the components of 64 Ori A, from which the long-period variation has been subtracted by means of the elements given in Table 3, plotted against phase measured from periastron in the short-period orbit. Velocities of Aa are shown as filled circles, while open circles indicate those of Ab. The curves represent the short-period elements of Table 3.

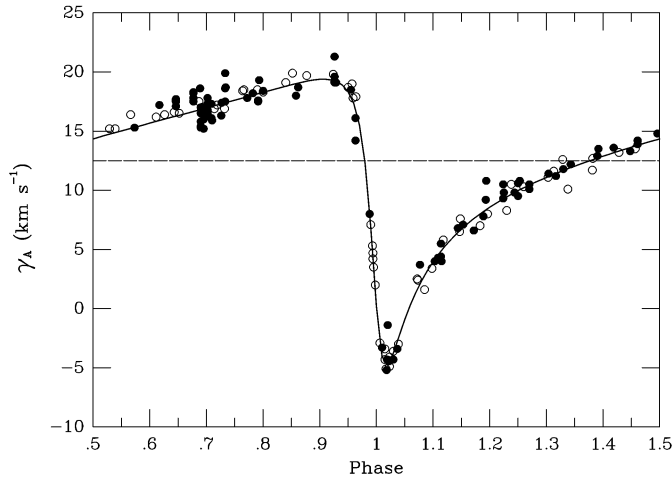


FIG. 2.—Long-period radial-velocity curve of 64 Ori from the elements given in Table 3, drawn through the center-of-mass velocities of the short-period pair, γ_A . Filled circles represent observations before apastron at JD 2,446,905 (1987 April 20), and open ones those obtained thereafter. Phases are measured from periastron, and the dashed line indicates the systemic radial velocity.

the system is now near maximum angular separation, making it currently resolvable with somewhat smaller aperture telescopes.

4. DYNAMICAL PARAMETERS

The most important advantage of Table 3 over Table IV of Fekel & Scarfe (1986) is the inclusion in the new table of the angular major semiaxis a , inclination i_L , and nodal position angle Ω of the long-period orbit. These alone are insufficient to determine uniquely the stellar masses and the system's orbital parallax; we still lack the mass ratio Q of the long-period orbit. However, we can write equations for all those quantities in terms of Q and known orbital elements, as follows. In each equation, the numerical constant is appropriate for use with the elements in the units listed in

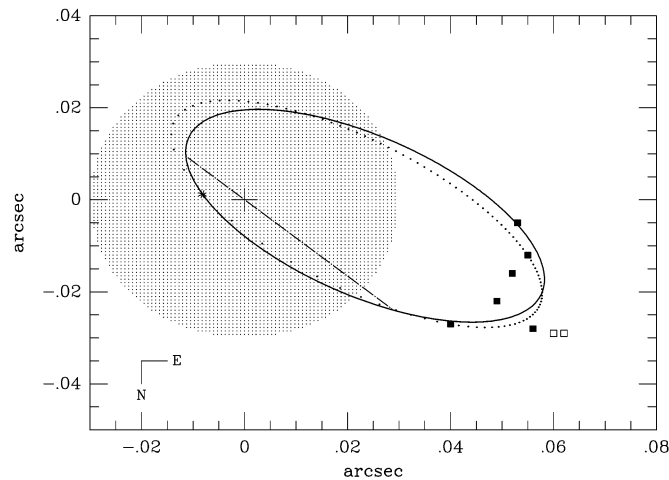


FIG. 3.—Speckle interferometric observations (filled squares for weight unity, open ones for weight 0.5) compared with the apparent ellipse (solid curve) that represents the elements obtained from the three-dimensional solution (Table 3). The position of component A is marked with a plus sign. The dot-dashed line is the line of nodes, and periastron is located by an asterisk. The dotted ellipse was computed with the visual elements of Mason (1997). The dotted area represents the 0.030 Rayleigh limit of a 4 m telescope.

Table 3 (days for P_L , which is also given in years in the table).

First, the system's parallax, π , is given by

$$\pi = 1.0880 \times 10^4 \left[\frac{a \sin i_L}{K_A P_L (1 - e_L^2)^{1/2}} \right] \left(\frac{Q}{1 + Q} \right). \quad (3)$$

Note that the numerator of the first fraction is *not* the spectroscopically determined product; instead, here a and i_L are both angular quantities, dependent upon the speckle data. The subscript L indicates an element of the long-period orbit and is used only for those elements for which either Table 3 or Table 4 also gives those of the short-period orbit. The mass of the distant companion, \mathcal{M}_B , is given in solar units by

$$\mathcal{M}_B = 1.0359 \times 10^{-7} P_L \left[\frac{K_A (1 - e_L^2)^{1/2}}{\sin i_L} \right]^3 \left(\frac{1 + Q}{Q} \right)^2. \quad (4)$$

The other two masses, \mathcal{M}_{Aa} and \mathcal{M}_{Ab} , are given respectively by

$$\mathcal{M}_{Aa} = \frac{\mathcal{M}_B}{Q(1 + q)}; \quad \mathcal{M}_{Ab} = q \mathcal{M}_{Aa}. \quad (5)$$

We used the parallax to determine absolute magnitudes for the system's components, applied bolometric corrections, and plotted (in Fig. 4) the locus of each star in the $[M_{bol}, \log(\mathcal{M}/\mathcal{M}_\odot)]$ -plane, for a range of plausible values of Q . To do so, however, it was necessary to obtain magnitude differences between the stars and individual color indices consistent with their spectral types and to ensure that those quantities combine in such a way as to match the observed colors, as was done to obtain Table V of Fekel & Scarfe (1986). We assumed that the system is unreddened, since the observed colors match the overall spectral type well and would not do so if significant reddening were present. As before, we adopted the Strömgen b magnitude difference

TABLE 4
DERIVED PROPERTIES

Parameter	Value
Orbital parallax (arcsec).....	0.00374 ± 0.00017
Distance (pc).....	268 ± 12
Distance modulus.....	7.14 ± 0.10
\mathcal{M}_{Aa} (\mathcal{M}_\odot).....	4.27 ± 0.35
\mathcal{M}_{Ab} (\mathcal{M}_\odot).....	3.88 ± 0.32
\mathcal{M}_B (\mathcal{M}_\odot).....	3.75 ± 0.27
$M_V(Aa)$	-1.30
$M_V(Ab)$	-0.32
$M_V(B)$	-0.50
$M_{bol}(Aa)$	-2.06
$M_{bol}(Ab)$	-0.93
$M_{bol}(B)$	-1.42
i_S (deg).....	23.00 ± 0.68
Angular momenta ($\mathcal{M}_\odot \text{ AU}^2 \text{ yr}^{-1}$):	
Inner orbit.....	16.3 ± 2.3
Outer orbit.....	133 ± 17
Coordinates of Right-Hand Pole of Outer Orbit	
Equatorial (J2000.0):	
<i>A</i>	1 ^h 11 ^m ± 15 ^m
<i>D</i>	52:9 ± 1:3
Galactic (deg):	
<i>l</i>	125.9 ± 2.3
<i>b</i>	-9.9 ± 1.3

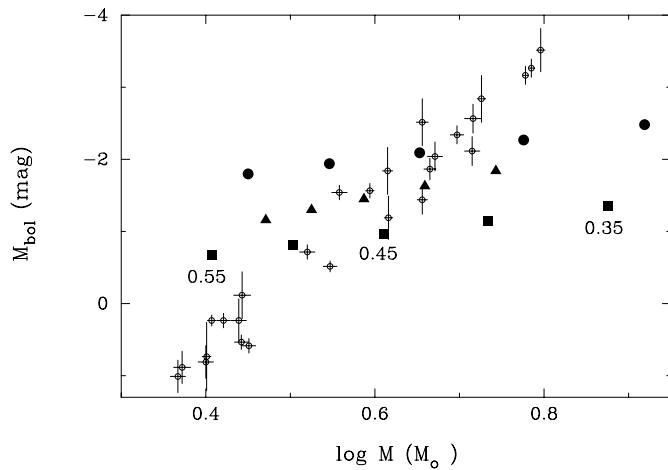


FIG. 4.— M_{bol} vs. $\log \mathcal{M}$ for values of Q in steps of 0.05, increasing from right to left. Filled circles are component Aa; squares are Ab; and triangles are B. Also plotted, as open circles with error bars in both coordinates, are data from the compilations of Andersen (1991) and Popper (1980).

between the components of the wide system measured by Africano et al. (1977) from their occultation observations and took it to represent ΔB since the stars' colors must all be very similar, as are their spectral types. This time, however, we used a magnitude difference between components Aa and Ab determined from seven of the KPNO CCD spectra obtained between 1994 and 1998. Specifically, the relative strengths of the three Fe II lines at 4489, 4508, and 4522 Å gave $\Delta m = 1.06 \pm 0.02$, while the much stronger line of Mg II at 4481 Å yielded 0.90 ± 0.02 . From these results, we adopted $\Delta m = 1.0 \pm 0.1$, which again we took to represent ΔB because of the similarity of the stars' colors and spectral types. Because this result is based on CCD spectra, we consider it to be more reliable than the value derived for ΔB photographically by Fekel & Scarfe (1986). We then used the tables of FitzGerald (1970) to convert between spectral types and colors and tried various combinations of the stars' types, within the range B7–B8 for Aa and Ab and B5–B6 for star B, found by Fekel & Scarfe (1986), in order to match the observed colors. The combination B7, B8, and B6 for Aa, Ab, and B, respectively, gave the best results, agreeing within 0.01 mag with the observed $U-B$ and $B-V$ indices for almost any choice of the observed magnitude differences within the uncertainties with which the latter are determined. We therefore adopted those types and the corresponding individual colors and obtained bolometric corrections from the colors using Table 3 of Flower (1996).

To determine the most plausible value of Q , we assumed that all three stars should obey the empirical mass-luminosity relationship, as defined by the stars with accurately known properties listed by Andersen (1991) and Popper (1980). Data for those objects are included in Figure 4, with Andersen's preferred over Popper's for systems in common. They populate a diagonal band about 1 mag wide, through which a line representing a fourth-power mass-luminosity law would pass almost centrally. Only for values of Q between 0.45 and 0.47 do all three components of 64 Ori fall within that band. We therefore adopt $Q = 0.46 \pm 0.01$ for the remainder of this paper and incorporate this estimate of the uncertainty of Q into that of all quantities dependent upon Q .

With Q as above, we obtain the masses and orbital parallax listed in Table 4. This table also includes the system's distance and distance modulus, as well as absolute magnitudes for the components, derived with the color indices and magnitude differences adopted above. We have not assigned uncertainties to those magnitudes. Beyond that from the distance modulus, the uncertainty in the absolute magnitude depends on the precision of our assignment of spectral types and magnitude differences and the conversion of those to colors and bolometric corrections, all of which are hard to quantify. Despite the system's distance and low Galactic latitude, there is no evidence for significant reddening of its light. Indeed, as already noted, any such reddening would make reconciliation of the spectral types and the observed colors almost impossible. Moreover, the orbital parallax agrees with the value of $0''.00305 \pm 0''.00096$ obtained for 64 Ori by *Hipparcos* (ESA 1997), within the latter's large error bar, but has an uncertainty less than one-fifth as big.

5. DISCUSSION

We now have sufficient information to determine the inclination of the short-period orbit i_s , using the expression

$$\sin^3 i_s = 1.0359 \times 10^{-7} \frac{P_S [(K_{Aa} + K_{Ab})(1 - e_s^2)]^{1/2}]^3}{\mathcal{M}_{Aa} + \mathcal{M}_{Ab}}. \quad (6)$$

The value of i_s is included in Table 4, and it confirms that the short- and long-period orbits are far from coplanar, as noted by Fekel & Scarfe (1986). Indeed the angle, j , between the orbital planes must lie in the range $41.3 < j < 87.3$, with an uncertainty of 2.3 at each end of that range.

We can also obtain information on the orbital angular momenta, even though our complete ignorance of the position angle of the node of the short-period orbit leaves indeterminate the orientation of its plane in space. For it, the magnitude of the angular momentum in units of $\mathcal{M}_\odot \text{AU}^2 \text{yr}^{-1}$ is given by

$$J_S = 2.011 \times 10^{-12} K_{Aa} K_{Ab} \times P_S^2 [(K_{Aa} + K_{Ab})(1 - e_s^2)]^3 \sin^{-5} i_s. \quad (7)$$

For the outer orbit, the magnitude of the angular momentum is given in the same units by

$$J_L = 2.011 \times 10^{-12} K_A^2 Q^{-1} \times P_L^2 [K_A(1 + Q^{-1})(1 - e_L^2)]^3 \sin^{-5} i_L. \quad (8)$$

Values of J_S and J_L are presented in Table 4. Their uncertainties are dominated by that of Q , through i_s in the case of J_S . The orientation of the vector J_L has been calculated in star-centered equatorial coordinates, A and D , with the formulas that follow:

$$-\sin D = \cos i_L \sin \delta + \sin i_L \cos \delta \sin \Omega, \quad (9)$$

$$\cos D \cos(A - \alpha) = -\cos i_L \cos \delta + \sin i_L \sin \delta \sin \Omega, \quad (10)$$

$$\cos D \sin(A - \alpha) = \sin i_L \cos \Omega. \quad (11)$$

These expressions are essentially those presented by Batten (1967), with the minor correction noted by Hans et al. (1979), but refer to the right-hand pole of the orbit, the true direction of the angular momentum vector. Because the speckle data cover only a short time interval, they have been assumed to refer to the equinox 1983.3, close to their

average date, and the values of i_L and Ω have been taken to be valid for that epoch. The system's equatorial coordinates, α and δ , for 1983.3 have therefore been used to obtain A and D for the same date. The results in Table 4, however, have been precessed to J2000.0. The same quantities, precessed this time to B1950.0, have been used to obtain the Galactic coordinates of the direction in space toward which the vector J_L points; these too are given in Table 4. The plane of the outer orbit is nearly normal to that of the Milky Way, and since that orbit's angular momentum dominates that of the system, the constant direction of the total angular momentum vector must not lie far from the Galactic plane.

In due course it may be possible to determine Q directly, either by astrometric means or by detection and measurement of the spectrum of B. This will permit a significant reduction in the uncertainties of the magnitudes of the angular momenta, as well as those of the other dynamical parameters of the system. It may also be possible to deduce the orientation of the inner orbit by resolving Aa and Ab with long-baseline interferometry or by observing the interaction between the angular momentum vectors caused by mutual gravitational perturbations. The timescale for the latter will be long, but since the ratio of the periods, 325, is somewhat smaller than in other systems we have studied, it may be possible to detect such changes during the next century. And since $J_L/J_S < 10$, both orbits will be perturbed.

Fekel & Scarfe (1986) noted that the projected rotational velocities of Aa and Ab are extremely low for early-type stars and estimated $v \sin i \leq 5 \text{ km s}^{-1}$ for each component. We have determined new values from two blue-wavelength CCD spectrograms using a procedure similar to that of Fekel (1997). For each component, the FWHM of several weak metal lines in the 4500 Å region was measured, and the results averaged. An instrumental broadening of 0.21 Å was removed from the measured mean broadening by taking the square root of the difference between the squares

of measurements of the stellar and comparison lines, resulting in the intrinsic stellar broadening. A calibration polynomial was used to convert this broadening in angstrom units into a total line broadening in units of kilometers per second, which was assumed to be the projected rotational velocity. We computed $v \sin i$ values of 3 km s^{-1} for both Aa and Ab with estimated errors being 2 km s^{-1} . Assuming that the orbital and rotational axes are parallel, we used $i = i_s = 23^\circ$ to obtain rotational velocities of $8 \pm 5 \text{ km s}^{-1}$ for both components. Since the two components are in a highly eccentric orbit, their rotational angular velocities will tend to synchronize with that of the orbital motion at periastron, a condition called pseudosynchronous rotation. With equation (42) of Hut (1981), we calculated a predicted pseudosynchronous period of 7.4 days. From the bolometric magnitudes in Table 4 and the effective temperature given by Flower (1996) for a star of the same color as 64 Ori Aa and Ab, we derived a mean value of those stars' radii near $4.2 R_\odot$. This in turn results in a predicted pseudosynchronous rotational velocity of 29 km s^{-1} . Thus, both Aa and Ab are rotating more slowly than the predicted pseudosynchronous velocity.

We are very grateful to Helmut Abt, who at our request obtained spectra in 1993 December and 1994 January, during the time of rapid velocity change in the long-period orbit. We thank Daryl Willmarth for measuring radial velocities from those spectra. We also thank Murray Fletcher for his skill and care in maintaining the ARCTURUS measuring machine, particularly after it was moved in 1997 from the DAO office building to the optical shop. This research has been supported in part by NASA grants NCC 5-228 and NCC 5-96, by NSF grant HRD 97-06268 to Tennessee State University, and in part by grants from the Natural Sciences and Engineering Research Council of Canada and from the University of Victoria.

REFERENCES

- Africano, J. L., Evans, D. S., Fekel, F. C., & Ferland, G. J. 1976, *AJ*, 81, 650
 Africano, J. L., Evans, D. S., Fekel, F. C., & Montemayor, T. 1977, *AJ*, 82, 631
 Andersen, J. A. 1991, *A&A Rev.*, 3, 91
 Batten, A. H. 1967, in *IAU Symp. 30, Determination of Radial Velocities and Their Applications*, ed. A. H. Batten & J. F. Heard (New York: Academic Press), 199
 Campbell, W. W. 1922, *PASP*, 34, 167
 ESA. 1997, *The Hipparcos and Tycho Catalogues* (ESA SP-1200) (Noordwijk: ESA)
 Fekel, F. C. 1997, *PASP*, 109, 514
 ———. 1999, in *ASP Conf. Ser. 185, Precise Stellar Radial Velocities*, ed. J. B. Hearnshaw & C. D. Scarfe (San Francisco: ASP), 378
 Fekel, F. C., Bopp, B. W., & Lacy, C. H. 1978, *AJ*, 83, 1445
 Fekel, F. C., & Scarfe, C. D. 1986, *AJ*, 92, 1162
 Fekel, F. C., Scarfe, C. D., Barlow, D. J., Duquennoy, A., McAlister, H. A., Hartkopf, W. L., Mason, B. D., & Tokovinin, A. A. 1997, *AJ*, 113, 1095
 FitzGerald, M. P. 1970, *A&A*, 4, 234
 Fitzpatrick, M. J. 1993, in *ASP Conf. Ser. 52, Astronomical Data Analysis Software and Systems II*, ed. R. J. Hanisch, R. V. J. Brissenden, & J. Barnes (San Francisco: ASP), 472
 Flower, P. J. 1996, *ApJ*, 469, 355
 Hans, E. M., Scarfe, C. D., Fletcher, J. M., & Morbey, C. L. 1979, *ApJ*, 229, 1001
 Hut, P. 1981, *A&A*, 99, 126
 Mason, B. D. 1997, *AJ*, 114, 808
 McAlister, H. A., & Hendry, E. M. 1982, *ApJS*, 48, 273
 Popper, D. M. 1980, *ARA&A*, 18, 115